Biosensors and Bioelectronics 54 (2014) 158–164

Contents lists available at ScienceDirect

Biosensors and Bioelectronics

journal homepage: www.elsevier.com/locate/bios

Carbon nanotube-based label-free electrochemical biosensor for sensitive detection of miRNA-24

Fengye Li [a], Jing Peng [a], Jingjing Wang [a], Hao Tang [a,*], Liang Tan [a], Qingji Xie [a], Shouzhuo Yao [a,b]

[a] Key Laboratory of Chemical Biology and Traditional Chinese Medicine Research (Ministry of Education), College of Chemistry and Chemical Engineering, Hunan Normal University, Changsha 410081, PR China
[b] State Key Laboratory of Chemo/Biosensing and Chemometrics, Hunan University, Changsha 410082, PR China

ARTICLE INFO

Article history:
Received 15 August 2013
Received in revised form
20 October 2013
Accepted 29 October 2013
Available online 7 November 2013

Keywords:
Multi-walled carbon nanotube modified electrode
miRNA-24
Label-free
Differential pulse voltammetry
Electrochemical biosensor

ABSTRACT

The recent findings concerning the function of microRNAs (miRNAs) and the relationship between miRNA levels with specific disease highlight the need for miRNA detection. In this work, multi-walled carbon nanotubes (MWCNTs), having shown great potential for biosensors, were used to develop a simple, label-free, and sensitive electrochemical biosensor for detection of miRNA-24 by monitoring the oxidation signal of guanine. The synthetic DNA probes, being complementary with miRNA-24, were immobilized onto the surface of MWCNT-modified glass carbon electrodes by covalent cross-linking. The probes were hybridized with different concentrations of miRNA-24. The formed hybrids on the electrode surface were evaluated by differential pulse voltammetry. The change of guanine oxidation signal was observed as a result of the hybridization between the probes and miRNA-24. Control experiments using the non-complementary miRNA-29 were performed to evaluate the selectivity. Numerous factors affecting probe immobilization, target hybridization, and nonspecific binding events were optimized. Under the optimal conditions, the proposed miRNA-24 biosensor exhibits good sensitivity (4.963 μA cm^{-2} $decade^{-1}$), low detection limit (1 pM), and good selectivity and reproducibility. The biosensor also has acceptable recovery for miRNA-24 detection in complex miRNA sample.

1. Introduction

MicroRNAs (miRNAs), as small RNA molecules (19–23 mers), can regulate the gene expression in plants and animals by binding to the 3′-untranslated region of messenger RNAs (Bartel, 2004), playing important roles in diverse biological processes including cell proliferation, fat metabolism, cell differentiation (Carthew, 2006; Zamore and Haley, 2005), etc. Moreover, recent studies have shown that miRNAs are linked with the onset of cancer and other diseases (Calin et al., 2002; Chan et al., 2005; Huang et al., 2008), which are dependent on the miRNA expression levels (Thum et al., 2008; Xiao and Rajewsky, 2009). To fully understand the roles of miRNAs, it is very important, therefore, to determine the miRNA expression levels. Many analytical methods for miRNA detection have been reviewed in the literatures (Cissell and Deo, 2009; Mariangelsde and Maria, 2011). Most present methods are relied on the hybridization between a target miRNA and a complementary DNA probe to produce a double-stranded helical molecule. The signals translated from the hybridization events can be detected in various analytical techniques such as optical and electrochemical measurements. Optical techniques generally include fluorescence spectroscopy (Bi et al., 2011; Calin and Croce, 2006; Chan et al., 2010; Cissell et al., 2008a, 2008c; Dodgson et al., 2012; Neely et al., 2006; Schneider et al., 2011; Shi and Chiang, 2005; Varallyay et al., 2008; Yin et al., 2012), bioluminescence spectroscopy (Cissell et al., 2008b), surface plasma resonance imaging measurement (Fang et al., 2006; Sipova et al., 2010), Raman scattering spectroscopy (Driskell et al., 2008), etc. For example, northern blotting and reverse transcriptase polymerase chain reaction (Shi and Chiang, 2005; Yu et al., 2011), as the most standardized and widely used methods for miRNA detection, usually involve the measurements of the change of fluorescence intensity before and after the hybridization between the target miRNA and the complementary DNA probe. These methods have intrinsic advantages along with some limitations. Northern blotting is very time-consuming and is semi-quantitative. Reverse transcriptase polymerase chain reaction is sensitive and rapid; however, it requires the addition of short primers, decreasing the stringency of the assay. Additionally, these methods require expensive commercial kits and the use of equipped laboratory with specialized and well-trained biologists.

Electrochemical analytic technique is attractive for miRNA detection due to simplicity, cost effectiveness, relatively high sensitivity,

* Corresponding author. Tel./fax: +86 731 88872046.
E-mail address: tanghao@hunnu.edu.cn (H. Tang).

0956-5663/$ - see front matter © 2013 Elsevier B.V. All rights reserved.
http://dx.doi.org/10.1016/j.bios.2013.10.061

and easy of miniaturization. Recently, some interesting electrochemical miRNA biosensors have been reported. A voltammetric miRNA biosensor is prepared using electrocatalytic $Ru(PD)_2Cl_2$, making it possible to conduct ultrasensitive miRNA detection (Gao and Yu, 2007). The inosine-substituted DNA capture probes are immobilized on the screen-printed graphite electrode by adsorption method and the probe modified electrode is used as a simple and sensitive platform for directly electrochemical detection of miRNA122 (Lusl et al., 2009). Based on the hybridized miRNA-template deposition of an insulating polymer film, Gao et al. (2013) make a simple and ultrasensitive impedimetric miRNA biosensor. The cumulative nature of the deposition process of the insulating film significantly enhances the sensitivity of the miRNA biosensor. Ren et al. (2013) design a highly sensitive and selective miRNA biosensor by using a duplex-specific nuclease, which initiates cleavage of the hybridized target miRNA to amplify the electrochemical signal. With the development of nanotechnology, nanomaterials, due to the specific physical and chemical properties, have been used for the construction of highly sensitive miRNA biosensors. The nanomaterials used involve OsO_2 nanoparticles (Gao and Yang, 2006), gold nanoparticles (Alhasan et al., 2012; Labib et al., 2013; Wang et al., 2012), silver nanoparticles or nanoclusters (Dong et al., 2012a; Liu et al., 2012), graphene oxide (Dong et al., 2012b; Tu et al., 2013; Yang et al., 2012), silicon nanowires (Dorvel et al., 2012; Zhang et al., 2009a), quantum dots (Cissell et al., 2008a; Zhang and Zhang, 2011), etc. For example, the isoniazid-capped OsO_2 nanoparticles are used to chemically amplify the hybridization signal of the immobilized capture probe and the target miRNA, greatly enhancing the detectability of miRNAs (Gao and Yang, 2006). A three-mode electrochemical biosensor based on hybridization, p19 protein binding, and protein displacement has been developed (Labib et al., 2013). Combined with gold nanoparticles, this three-mode electrochemical biosensor is successfully used for direct detection of three kinds of miRNAs. Fan et al. (2007) prepare a sensitive electric biosensor array based on the hybridized miRNA-guided in situ formation of polyaniline nanowires, leading to significant enhancement of the signal when the target miRNA is present in the sample solution. These results suggest that nanomaterials have great potential for highly sensitive detection of miRNAs.

Carbon nanotubes (CNTs), as a typical one-dimensional nanomaterial, possess unique mechanical, electronic, and chemical properties, which spawn a huge field of scientific research. In the past decade, many works exhibit that CNTs have advantages such as small size with large surface area, excellent electron transfer ability, and easy of biomolecule immobilization, rendering CNTs promising applications in biosensors (Liu et al., 2009; Trojanowicz, 2006; Wang and Lin, 2008). To the best of our knowledge, however, the use of CNTs for miRNA detection has not been investigated. In this paper, we proposed a simple, label-free, and sensitive CNT-based electrochemical biosensor for miRNA detection (Fig. 1). The electrochemical detection of miRNAs is based on the guanine oxidation consequent to the hybridization between the target miRNA and the complementary DNA capture probe (Lusl et al., 2009). The oxidation of guanine before and after hybrid formation generates voltammetric signal change, which is measured by differential pulse voltammetry (DPV). CNTs have excellent electrochemical property for guanine oxidation, already described for nucleic acid detection (Ariksoysal et al., 2005; Li et al., 2003; Palecek and Bartosik, 2012). The use of CNTs may enhance the sensitivity of guanine determination, resulting in improved analytical performance of the electrochemical miRNA biosensor. Moreover, the proposed biosensor involved no labels, external indicators, and complicated bio/chemical reactions, making the detection simple and cost-effective. As a model case, we used the miRNA-24, which plays important roles in cell proliferation (Cheng et al., 2005; Lagos-Quintana et al., 2001) and cancer cell differentiation (Cameron et al., 2008). The CNT-based biosensor exhibits good analytical properties (high sensitivity, low detection limit, and good selectivity and reproducibility) for miRNA-24 detection.

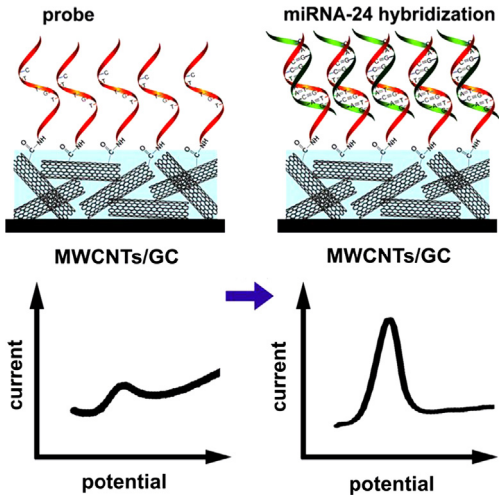

Fig. 1. The scheme demonstrating the principle of miRNA-24 detection by MWCNT-based electrochemical biosensor.

2. Material and methods

2.1. Chemicals and Instruments

Multi-walled CNTs (MWCNTs, out diameter, 10–20 nm; length, 5–15 μm; purity >95%) were purchased from Shenzhen Nano-Technologies Port Co., Ltd. (China). Guanine was obtained from Jiehui Biotechnology Co., Ltd. (Changsha) and used as received. The stock solution of guanine (10 mM) was prepared by 0.1 M NaOH aqueous solution and was stored at 4 °C for future use. 1-Ethyl-3-(3-dimethylaminopropyl) carbodiimide (EDC, hydrochloride form) and *N*-hydroxy-succinimide (NHS) were purchased from Bio Basic Inc. and Sinopharm Chemical Reagent Co., Ltd. The synthetic miRNA-24, 5′-amine terminated DNA capture probe, miRNA-29, and central single base-mismatched miRNA-24 were purchased from Invitrogen Corporation (Life Technologies, Shanghai). The base sequences of the DNA capture probe and the miRNAs were as follows:

DNA probe 5′-NH_2-C TGT TCC TGC TGA ACT GAG CCA-3′
miRNA-24 5′-UGG CUC AGU UCA GCA GGA ACA G-3′
miRNA-29 5′-UAG CAC CAU CUG AAA UCG GUU A-3′
Central single base-mismatched miRNA-24 5′-UGG CUC AGU UGA GCA GGA ACA G-3′

The total RNA (571.5 μg mL^{-1}) samples were kindly provided by College of Biology, Hunan University. The total RNA was extracted from cultured Huh 7.5 cells by TRIZOL reagent (Invitrogen Corporation, Life Technologies, Shanghai) according to manufacturer's recommended protocol. UltraPure™ diethyl pyrocarbonate (DEPC)-treated water was purchased from Invitrogen Corporation (Life Technologies, Shanghai) and was used for miRNA-24 detection. Phosphate buffered saline (PBS, 0.1 M, pH 7.38) solutions were used in the experiments. Sodium citrate for preparation of saline-sodium citrate (SSC) solutions, sodium dodecyl sulfate (SDS), and all other reagents were of analytical grade or better. Milli-Q ultrapure water (>18 MΩ cm, Milli-pore Co., Ltd.) and fresh prepared solutions were used throughout.

A CHI600C electrochemical workstation (CH Instruments Co.) and a conventional three-electrode electrolytic cell were used in

the electrochemical experiments. The glass carbon (GC, diameter 3 mm) electrode modified with carboxylated MWCNTs was served as the working electrode. The reference electrode was a KCl-saturated calomel electrode (SCE) and a platinum wire served as a counter electrode. All potential values given below are referred to the SCE electrode. Unless otherwise specified, experiments were performed at room temperature. The measurements were repeated at least three times and the means of measurements were presented with the standard deviations (SD).

2.2. Preparation of MWCNT modified GC electrode and capture probe immobilization

The received MWCNTs were firstly treated by mixed acids (concentrate $H_2SO_4+HNO_3$, v/v 3:1) for 24 h to prepare carboxylated MWCNTs. The detail procedures are according to the previous literature (Li et al., 2011). The MWCNT aqueous suspension (1 mg mL^{-1}) was prepared for future use (hereafter, unless otherwise specified, the MWCNTs were referred to carboxylated MWCNTs). The MWCNT modified GC (MWCNTs/GC) electrodes were prepared by drop coating of MWCNT aqueous suspension on the GC electrode surface. Before MWCNT modification, the GC electrode was pretreated by the following steps. The GC electrode was firstly polished with $5^{\#}$ grit paper and Al_2O_3 powder (0.3–0.5 μm) in turn, and then rinsed with ultrapure water. After that, the GC electrode was sonicated in ethanol and acetone for 5 min, followed by a careful rinse with copious ultrapure water. Finally, the as-pretreated GC electrode was cycled in the potential range of 0–1.0 V at a scan rate of 100 mV s^{-1} in 0.1 M H_2SO_4 aqueous solution for sufficient cycles until cyclic voltammograms were reproducible. After rinsing with copious ultrapure water, the GC electrode was characterized by cyclic voltammetry in the potential range of −0.1 to 0.5 V at a scan rate of 50 mV s^{-1} in 0.1 M Na_2SO_4 aqueous solutions containing 2 mM $K_4[Fe(CN)_6]$. For preparation of MWCNTs/GC electrode, MWCNT aqueous suspensions (different volumes) were drop coated onto the surface of pretreated GC electrode, followed by drying under infrared lamp.

The capture probes were immobilized onto the surface of the MWCNTs/GC electrode by covalent binding between 5′-amine group of the capture probe and the carboxyl group of the MWCNTs using EDC and NHS as coupling reagents. The MWCNTs/GC electrode prepared was firstly immersed into 150 μL of 0.4 M EDC and 0.1 M NHS aqueous solutions for 5 min, and then rinsed with copious ultrapure water. The activated MWCNTs/GC electrode was immersed into 150 μL of 1 μM capture probe ultrapure water solution for 3 h. Successive washing steps were applied onto the probe/MWCNTs/GC electrode to minimize the nonspecific adsorption: 1 × SSC, 0.1% SDS, and DEPC water in turn for 5 min.

2.3. Electrochemical detections

The electrochemical oxidation of guanine at the MWCNTs/GC electrode was investigated by DPV in PBS containing guanine over the potential range of 0.5–0.9 V. The MWCNTs/GC electrode was immersed in the guanine PBS solution for 5 min before DPV measurement. Fresh electrodes and guanine PBS solution were used for the independent measurements. The DPV parameters are as follows: potential increment, 4 mV; amplitude, 50 mV; pulse period, 0.2 s. For comparison, the electrochemical oxidation of guanine at GC electrode was also investigated.

For the miRNA-24 hybridization and electrochemical detection, the probe/MWCNTs/GC electrode was dipped into 150 μL of DEPC water containing different concentration of miRNA-24. The hybridization was allowed to proceed for 1 h at room temperature and at 50 °C as well. After successive washing with 1 × SSC, 0.1% SDS, and DEPC water in turn for 5 min, the guanine oxidation signal of the probe+miRNA-24/MWCNTs/GC electrode was measured by DPV in blank PBS over the potential range of 0.5–1.0 V. The DPV parameters are as follows: potential increment, 4 mV; amplitude, 50 mV; pulse period, 0.2 s. The guanine oxidation signal of the probe/MWCNTs/GC electrode was also measured as a background. The procedures are similar with the probe+miRNA-24/MWCNTs/GC electrode. To test the specificity of the assay, the synthetic oligonucleotides of miRNA-29 was used as control. The capacity of the probe/MWCNTs/GC electrode to discriminate the single base-mismatch of miRNAs was also investigated by using the central single base-mismatched miRNA-24. Moreover, the analytical applicability of the prepared probe/MWCNTs/GC electrode in complex sample was evaluated by standard addition method using total RNA samples that extracted from Huh 7.5 cells.

3. Results and discussion

3.1. Electrochemical oxidation of guanine at the MWCNTs/GC electrode

To confirm the feasibility of the MWCNT-based electrochemical biosensor for miRNA-24 detection, the electrochemical property of the MWCNTs/GC electrode for guanine oxidation was firstly investigated. The electrochemical oxidation of guanine at carbon-based material electrodes is irreversible, pH dependent, and the electron transfer process occurs in consecutive steps with the formation of very strongly absorbed oxidation products and dimers on the electrode surface (Abbaspour and Noori, 2008; Li et al., 2010; Oliveira-Brett et al., 2002). Moreover, guanine adsorption on pyrolytic graphite and GC electrodes has also been reported (Oliveira-Brett et al., 2002). Considering the effects of these factors, the MWCNTs/GC and GC electrodes were immersed in PBS containing guanine for 5 min before DPV scan and the electrodes underwent only once DPV measurement. Fresh electrodes and guanine PBS solution were used for the independent measurements. Fig. 2A shows the differential pulse voltammograms of guanine at the GC and MWCNTs/GC electrodes. At the GC electrode, guanine exhibits an anodic peak at about 0.64 V and the peak current density (i_{peak}) is 55.8 μA cm^{-2}. For the MWCNTs/GC electrode, the peak potential of guanine oxidation is about 0.66 V, showing a little positive shift than that at the GC electrode. This is accordant with other work (Wang et al., 2003). The i_{peak} of guanine oxidation at the MWCNTs/GC electrode reaches 152.8 μA cm^{-2}, which is about 2.8 times as large as that at the GC electrode. The modification of the GC electrode by MWCNTs facilitates larger surface coverage, providing enhanced adsorption of guanine, and consequently offers larger i_{peak}. This improved guanine oxidation signal by using the MWCNTs/GC electrode may promote the sensitivity of miRNA-24 detection. On the other hand, the effect of MWCNT loading mass on the i_{peak} of guanine oxidation at the MWCNTs/GC electrode was evaluated (shown in Fig. 2B). The MWCNTs/GC electrode shows the largest i_{peak} at 42.4 μg cm^{-2} of MWCNT loading and further increase of MWCNT loading mass results in the decrease of the i_{peak}. When the loading mass is larger than 42.4 μg cm^{-2}, the aggregation among MWCNTs occurs and thus decreases the active surface area of the MWCNTs/GC electrode for electrochemical oxidation of guanine. Therefore, the GC electrode needs to be modified with the MWCNTs at an optimal loading mass to obtain maximum improvement of guanine electrochemical property. In the following experiments, the MWCNT loading mass is selected to be 42.4 μg cm^{-2}.

3.2. DPV characterization of the probe/MWCNTs/GC electrode before and after hybridization

The label-free detection of miRNA-24 was performed by DPV transduction of the hybridization between the immobilized

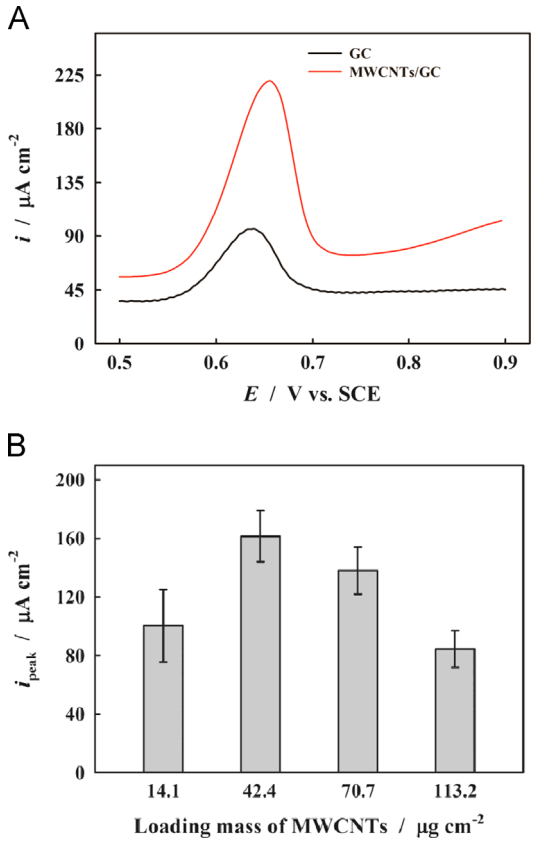

Fig. 2. (A) The differential pulse voltammograms of guanine at the GC (black line) and the MWCNTs/GC (red line) electrodes in PBS (pH 7.38) containing 10 μM guanine. The loading mass of MWCNTs is 70.7 μg cm^{-2}. (B) The effect of MWCNT loading mass on the peak current density of guanine at the MWCNTs/GC electrode in PBS (pH 7.38) containing 10 μM guanine (For interpretation of the references to color in this figure legend, the reader is referred to the web version of this article).

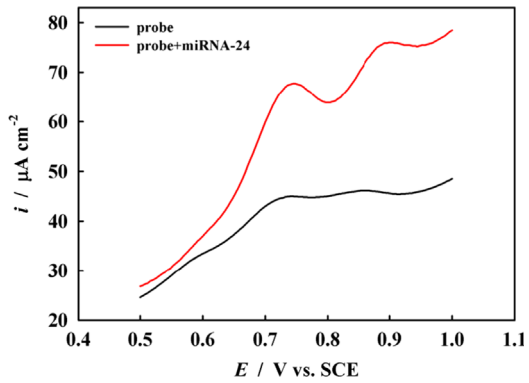

Fig. 3. Typical DPV curves of the probe/MWCNTs/GC electrode before (black line) and after (red line) hybridization with miRNA-24. Electrolyte, blank PBS (pH 7.38); the concentrations of the probe and miRNA-24 are 1 μM and 10 nM (For interpretation of the references to color in this figure legend, the reader is referred to the web version of this article).

capture probes and the target miRNA-24. The guanine signal (i_{peak}) of the immobilized capture probes is used as background and the change of the guanine signal after hybridization thus shows the target miRNA-24. The DPV technique provides lower detection limits than the ones obtained by potentiometric stripping analysis and square wave voltammetry (Palecek and Fojta, 1994). Fig. 3 shows the typical DPV curves of the probe/MWCNTs/GC electrode before (black line) and after (red line) hybridization with miRNA-24. For the probe/MWCNTs/GC electrode, two anodic peaks are observed at about 0.74 and 0.86 V, which are corresponding to the electrochemical oxidation of guanine and adenine (Abbaspour and Noori, 2008). In contrast to guanine oxidation at the MWCNTs/GC electrode (Fig. 2A), the guanine peak potential of the probe/MWCNTs/GC electrode shifts positively about 100 mV, indicating the guanine in the DNA probes is more difficult to be electrochemically oxidized than that in aqueous solution. After the miRNA-24 hybridization, the probe+miRNA-24/MWCNTs/GC electrode exhibits significant enhancement of the guanine oxidation signal (Fig. 3, red line). The change of peak current density (Δi_{peak}) of guanine oxidation before and after hybridization reaches about 7.63 μA cm^{-2}. The peak potential (about 0.75 V) of the probe+miRNA-24/MWCNTs/GC electrode, however, shows a slightly positive shift in contrast to the probe/MWCNTs/GC electrode. The immobilized probe DNA may lie flat down or wrap around the MWCNT surface due to the flexible property of ssDNA and the interaction between ssDNA and CNTs (Zhang et al., 2009b). Additionally, the guanine base in the probe DNA is highly exposed. These two factors should facilitate the guanine oxidation. Interaction between the probe DNA and the complementary miRNA-24 could peel the probe DNA off the MWCNT surface (Zhang et al., 2009b) and the structure of the double helix is more rigid than the single helix (Erdem et al., 2006), which makes the probe+miRNA-24 hybrids hard to wrap around MWCNTs. Furthermore, in the probe+miRNA-24 hybrids, the formed pairing of guanine and cytosine bases is located in the center of the double helix. Therefore, the formation of the probe+miRNA-24 hybrids leads to the orientation changes of the probe DNA and guanine base. These orientation changes may make the guanine more difficult to be electrooxidized, and consequently the peak potential of guanine oxidation shifts slightly positive at the probe+miRNA-24/MWCNTs/GC electrode. Based on the results of Fig. 3, it is feasible to determine miRNA-24 by the proposed MWCNT-based electrochemical biosensor.

3.3. Optimization of EDC activation time, hybridization temperature and time, and washing step

To obtain optimal conditions for miRNA-24 detection, the effects of EDC activation time, hybridization temperature and time, and washing steps on the i_{peak} of guanine oxidation in the probe/MWCNTs/GC and probe+miRNA-24/MWCNTs/GC electrodes were investigated in detail. The capture probe was covalently immobilized onto the MWCNTs/GC electrode surface using EDC and NHS as coupling reagents. The EDC activation time was firstly optimized. The result of Fig. 4A exhibits that 5 min of EDC activation time result in the maximum i_{peak} in the probe/MWCNTs/GC electrodes. The intermediate produced by reaction between EDC and carboxyl group is susceptible to hydrolysis although NHS can stabilize the intermediate. The longer activation time (> 5 min) will thus decrease the efficiency of the cross-linking reaction, resulting in the decrease of the probe immobilization. The different temperature (room temperature and 50 °C) and time conditions (10–80 min) were used for the hybridization. Hybridization at room temperature produces a little increase of the guanine i_{peak} at different miRNA-24 concentrations (Fig. 4B). However, hybridization time has significant effect on the i_{peak} of guanine oxidation (Fig. 4C). The guanine signal increases with the increase of hybridization time (10–60 min) and 60 min of hybridization produces the largest i_{peak}. But the prolonged time (80 min) significantly decreases the response. Optimal hybridization time is necessary to maximize the hybrid formation between the probe and the miRNA-24; however, miRNAs are susceptible to degrade because of the ubiquitously present RNases (although DEPC water was used during hybridization). Thus, the probe+miRNA-24/MWCNTs/GC electrodes exhibit decreased guanine signal when the hybridization time extends to 80 min. The nonspecific adsorption of capture probe and target miRNAs on the electrode surface is an

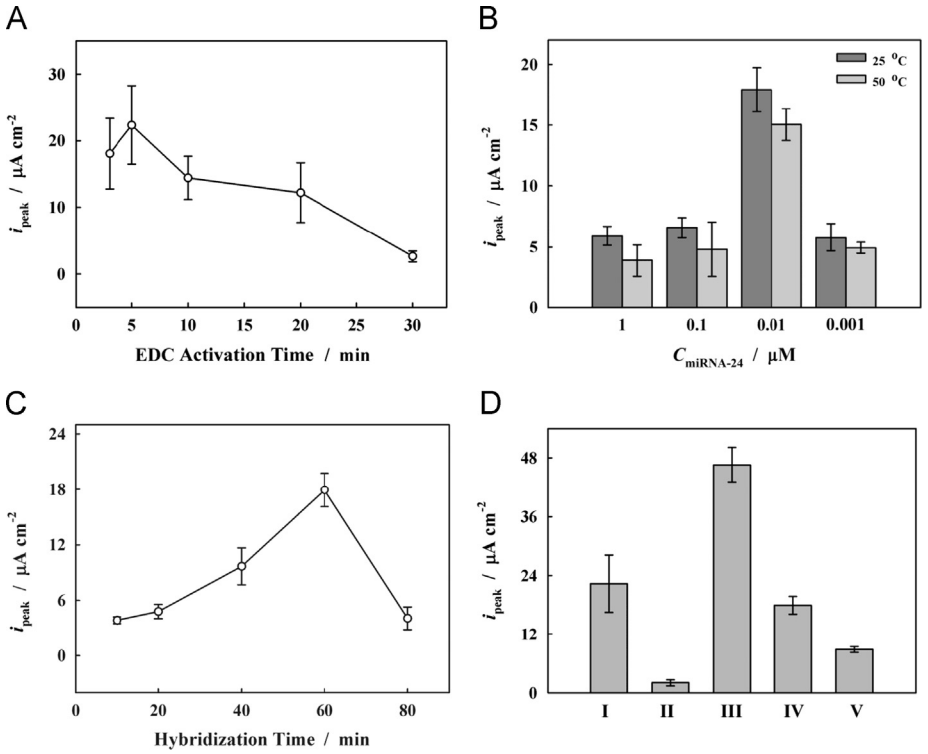

Fig. 4. The effect of the EDC activation time (A) on i_{peak} of guanine oxidation at the probe/MWCNTs/GC electrodes. The effects of hybridization temperature (B) and time (C) on i_{peak} of guanine oxidation at the probe+miRNA-24/MWCNTs/GC electrodes. After probe immobilization (A–C), the probe/MWCNTs/GC electrodes were rinsed with ultrapure water; after hybridization (B and C), the probe+miRNA-24/MWCNTs/GC electrodes were rinsed with SSC, SDS, and DEPC water in turn. (D) The effect of washing steps on i_{peak} of guanine oxidation at the probe/MWCNTs/GC (I and II) and probe+miRNA-24/MWCNTs/GC (III–V) electrodes. After the probe immobilization, the electrodes were rinsed with ultrapure water (I, III, and IV) and SSC, SDS, and DEPC water (II and V); after the miRNA-24 hybridization, the electrodes were rinsed with ultrapure water (III) and SSC, SDS, and DEPC water (IV and V). The concentration of miRNA-24 is 10 nM (C and D).

important factor that affects the miRNA detection. In our experiments, washing steps by using SSC, SDS, and DEPC water were performed to minimize the nonspecific adsorption. SSC and SDS have been used successfully to suppress the nonspecific binding effects (Ariksoysal et al., 2005; Lusl et al., 2009). The results (Fig. 4D) clearly demonstrate that the i_{peak} of guanine oxidation in the probe/MWCNTs/GC and probe+miRNA-24/MWCNTs/GC electrodes greatly reduces after the electrodes are successively rinsed with SSC, SDS, and DEPC water. In the following experiments, the miRNA-24 detections are performed under the optimal conditions.

3.4. Analytical properties of the probe/MWCNTs/GC electrode for miRNA-24 detection

To test the selectivity and the capacity of discriminating the single base-mismatched miRNAs of the assay, the miRNA-29 and the central single base-mismatched miRNA-24 were used as control. Fig. 5 shows the responses of the probe/MWCNTs/GC electrodes to different miRNAs. The Δi_{peak} obtained from the hybridization with 10 nM of miRNA-29 (Fig. 5, II) is very little in contrast to the probe, indicating that the hybridization is not accomplished with a non-complementary sequence and the assay has good selectivity. The little increase of i_{peak} after hybridization with the miRNA-29 is attributed to the nonspecific adsorption of miRNA-29 on the electrode surface. The nonspecific adsorption is effectively suppressed by washing steps using SSC and SDS (Ariksoysal et al., 2005) but it cannot be completely eliminated. After hybridization with 10 nM of the central single base-mismatched miRNA-24 (Fig. 5, III), however, the electrodes exhibit relatively large Δi_{peak}, suggesting the assay cannot discriminate the central single base-mismatch of miRNAs. The mismatched

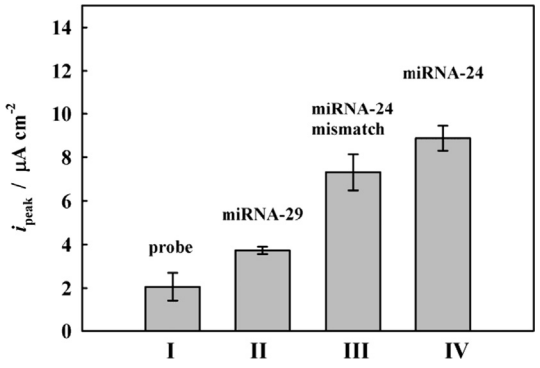

Fig. 5. Responses of the probe/MWCNTs/GC electrodes to three kinds of miRNAs. The concentrations of the miRNAs are all 10 nM.

single base is centrally located in the sequence, providing half of the sequence that hybridizes with the probe DNA, and hence results in relatively large response. However, in general, the probability that the miRNA-24 and its central single base-mismatched sequence are simultaneously present should be very low. Therefore, our test will detect the miRNA-24 from complex sample with good specificity. On the other hand, the reproducibility was investigated. Samples (10 nM) were detected by five miRNA-24 biosensors, giving a relative standard deviation (RSD) of 6.5%. The results reveal that the biosensor has satisfied reproducibility.

Fig. 6 shows the relationship between the Δi_{peak} and the logarithm of miRNA-24 concentration ($\log C_{miRNA-24}$). In the range of 1 pM to 1 nM, the Δi_{peak} progressively increases with the increase of miRNA-24 concentration, although the enhancement is not so significant. The Δi_{peak} exhibits obvious increase with further increase of miRNA-24 concentration (1–10 nM) and the largest value is

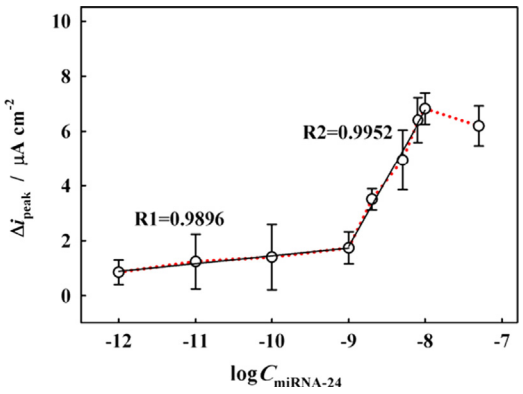

Fig. 6. The dependence of Δi_{peak} on the log $C_{miRNA-24}$.

observed when 10 nM of the target is used. However, at 50 nM concentration of the target, the amplitude of the Δi_{peak} starts to decrease. The Δi_{peak} shows different tendency with the increase of miRNA-24 concentration, which is probably due to the amount of the probe+miRNA-24 hybrids on the electrode surface and the hybridization efficiency. In the low miRNA-24 concentration range (1 pM to 1 nM), few miRNA-24 molecules are present in the hybridization solution, resulting in a few of probe+miRNA-24 hybrids formed at the electrode surface, and consequently the Δi_{peak} exhibits a slightly increase. With the increase of miRNA-24 concentration (1–10 nM), it produces more probe+miRNA-24 hybrids. On the other hand, as discussed in Section 3.2, the interaction between the probe DNA and the miRNA-24 target could induce a change of the probe orientation, which may provide a better accessibility of the probe and hence improve the hybridization efficiency. This effect may become strong at large miRNA-24 concentration (>1 nM). However, too large of miRNA-24 concentration (50 nM) leads to a decrease of Δi_{peak}, which is probably the steric interaction and electrostatic repulsion between the probe and the miRNA-24 target that reduce the hybridization efficiency. In fact, the interaction between the probe DNA and miRNAs should be complicated and affected by many factors including the conformation and length of the probe DNA, the concentration of target (Jayaraman et al., 2007; Maskos and Southern, 1992; Riccelli et al., 2001; Shchepinov et al., 1997), etc. Future experiments are needed to reveal the effects of these factors so as to develop miRNA biosensors with high performance. The Δi_{peak}–log $C_{miRNA-24}$ curve shows two linear ranges with different slopes. The regression equations in the ranges of 1 pM to 1 nM and 1–10 nM can be obtained and expressed as $\Delta i_{peak}=4.272+0.2822$ log $C_{miRNA-24}$ and $\Delta i_{peak}=46.47+4.963$ log $C_{miRNA-24}$. The two linear curves have the slopes of 0.2822 and 4.963 μA cm^{-2} decade^{-1} (the sensitivity of the miRNA-24 biosensor) and the correlation coefficients are 0.9896 and 0.9952. The detection limit is 1 pM ($S/N=3$), which is lower than that of the existing analog using screen-printed electrodes modified with electrodeposited inosine-substituted capture probes for miRNA-122 detection by ca. 3 orders (Lusl et al., 2009), and better than or comparable with those reported previously using other protocols with signal amplification for various miRNA detection (Gao and Yu, 2007; Qavi et al., 2011; Sipova et al., 2010; Wang and Zhang, 2012). The detection limits of several electrochemical or fluorescence biosensors for different miRNA detection are listed in Table S1 (Supporting information). The analytical applicability of the proposed miRNA-24 biosensor was evaluated by the standard addition method. The developed miRNA-24 biosensor was used to detect the miRNA-24 in the total RNA samples and the recovery (addition of miRNA-24, 2 nM; $n=3$) is 108.9% with a RSD of 15.6%. The acceptable recovery and RSD suggest that the miRNA-24 biosensor has potential application in complex miRNA samples.

4. Conclusions

We have developed a simple, cost-effective, and sensitive MWCNT-based electrochemical miRNA-24 biosensor. Under optimal conditions, the prepared probe/MWCNTs/GC electrodes have good sensitivity, low detection limit, good specificity as well acceptable recovery and reproducibility for miRNA-24 determination. In contrast to the existing methods for miRNA detection, the MWCNT-based biosensor is directly based on the signal change of guanine oxidation, which eliminates the need for specific capture probe, hybridization labels, and the use of an expensive kit or of toxic chemicals. The proposed MWCNT-based biosensor may find wide applications in the routine detection of miRNAs by a simple way.

Acknowledgments

This work was supported by the National Natural Science Foundation of China under grants (21275050, 21145001, 20705008 and 20905025), the Hunan Provincial Natural Science Foundation of China (13JJ1016), the Scientific Research Fund of Hunan Provincial Education Department (13A053), and the Aid Program for Science and Technology Innovative Research Team in Higher Educational Institutions of Hunan Province.

Appendix A. Supporting information

Supplementary data associated with this article can be found in the online version at http://dx.doi.org/10.1016/j.bios.2013.10.061.

References

Abbaspour, A., Noori, A., 2008. Analyst 133, 1664–1672.
Alhasan, A.H., Kim, D.Y., Daniel, W.L., Watson, E., Meeks, J.J., Thaxton, C.S., Mirkin, C.A., 2012. Anal. Chem. 84, 4153–4160.
Ariksoysal, D.O., Karadeniz, H., Erdem, A., Sengonul, A., Sayiner, A.A., Ozsoz, M., 2005. Anal. Chem. 77, 4908–4917.
Bartel, D., 2004. Cell 116, 281–297.
Bi, S., Zhang, J., Hao, S., Ding, C., Zhang, S., 2011. Anal. Chem. 83, 3696–3702.
Calin, G.A., Croce, G.M., 2006. Nat. Rev. Cancer 6, 857–866.
Calin, G.A., Dumitru, C.D., Shimizu, M., Bichi, R., Zupo, S., Noch, E., Aldler, H., Rattan, S., Keating, M., Rai, K., Rassenti, L., Kipps, T., Negrini, M., Bullrish, F., Croce, C.M., 2002. Proc. Natl. Acad. Sci. USA 99, 15524–15529.
Cameron, J.E., Fewell, C., Yin, Q., McBride, J., Wang, X., Lin, Z., Flemington, E.K., 2008. Virology 382, 257–266.
Carthew, R.W., 2006. Curr. Opin. Genet. Dev. 16, 203–208.
Chan, H.-M., Chan, L.-S., Wong, R.N.-S., Li, H.-W., 2010. Anal. Chem. 82, 6911–6918.
Chan, J.A., Krichevsky, A.M., Kosik, K.S., 2005. Cancer Res. 65, 6029–6033.
Cheng, A.M., Byrom, M.W., Shelton, J., Ford, L.P., 2005. Nucleic Acids Res. 33, 1290–1297.
Cissell, K.A., Campbell, S., Deo, S.K., 2008a. Anal. Bioanal. Chem. 391, 2577–2581.
Cissell, K.A., Deo, S.K., 2009. Anal. Bioanal. Chem. 394, 1109–1116.
Cissell, K.A., Rahimi, Y., Shrestha, S., Deo, S.K., 2008b. Bioconjug. Chem. 20, 15–19.
Cissell, K.A., Rahimi, Y., Shrestha, S., Junt, E.A., Deo, S.K., 2008c. Anal. Chem. 80, 2319–2325.
Dodgson, B.J., Mazouchi, A., Wegman, D.W., Gradinaru, C.C., Krylov, S.N., 2012. Anal. Chem. 84, 5470–5474.
Dong, H., Jin, S., Ju, H., Hao, K., Xu, L.-P., Lu, H., Zhang, X., 2012a. Anal. Chem. 84, 8670–8674.
Dong, H., Zhang, J., Ju, H., Lu, H., Wang, S., Jin, S., Hao, K., Du, H., Zhang, X., 2012b. Anal. Chem. 84, 4587–4593.
Dorvel, B.R., Reddy, B., Go, J., Duarte Guevara, C., Salm, E., Alam, M.A., Bashir, R., 2012. ACS Nano 6, 6150–6164.
Driskell, J.D., Seto, A.G., Jones, L.P., Jokela, S., Dluhy, R.A., Zhao, Y.P., Tripp, R.A., 2008. Biosens. Bioelectron. 24, 917–922.
Erdem, A., Papakonstantinou, P., Murphy, H., 2006. Anal. Chem. 78, 6656–6659.
Fan, Y., Chen, X., Trigg, A.D., Tung, C.-h., Kong, J., Gao, Z., 2007. J. Am. Chem. Soc. 129, 5437–5443.
Fang, S., Lee, H.J., Wark, A.W., Corn, R.M., 2006. J. Am. Chem. Soc. 128, 14044–14046.
Gao, Z., Deng, H., Shen, W., Ren, Y., 2013. Anal. Chem. 85, 1624–1630.
Gao, Z., Yang, Z., 2006. Anal. Chem. 78, 1470–1477.
Gao, Z., Yu, Y.H., 2007. Biosens. Bioelectron. 22, 933–940.

Huang, Q., Gumireddy, K., Schrier, M., le Sage, C., Nagel, R., Nair, S., Egan, D.A., Li, A., Huang, G., Klein Szanto, A.J., Gimotty, P.A., Katsaros, D., Coukos, G., Zhang, L., Pure, E., Agami, R., 2008. Nat. Cell Biol. 10, 202–210.
Jayaraman, A., Hall, C.K., Genzer, J., 2007. J. Chem. Phys. 127144912
Labib, M., Khan, N., Ghobadloo, S.M., Cheng, J., Pezacki, J.P., Berezovski, M.V., 2013. J. Am. Chem. Soc. 135, 3027–3038.
Lagos-Quintana, M., Rauhut, R., Lendeckel, W., Tuschl, T., 2001. Science 294, 853–858.
Li, C., Yang, K., Zhang, Y., Tang, H., Yan, F., Tan, L., Xie, Q., Yao, S., 2011. Acta Biomater. 7, 3070–3077.
Li, J., Ng, H.T., Cassell, A., Fan, W., Chen, H., Ye, Q., Koehne, J., Han, J., Meyyappan, M., 2003. Nano Lett. 3, 597–602.
Li, Q., Batchelor-McAuley, C., Compton, R.G., 2010. J. Phys. Chem. B 114, 7423–7428.
Liu, Y.-Q., Zhang, M., Yin, B.-C., Ye, B.-C., 2012. Anal. Chem. 84, 5165–5169.
Liu, Z., Tabakman, S., Welsher, K., Dai, H.J., 2009. Nano Res. 2, 85–120.
Lusl, E.A., Passamano, M., Guarasclo, P., Scarpa, A., Schlavo, L., 2009. Anal. Chem. 81, 2819–2822.
Mariangelsde, P.-S., Maria, C.R., 2011. Anal. Chim. Acta 699, 134–152.
Maskos, U., Southern, E.M., 1992. Nucleic Acids Res. 20, 1675–1678.
Neely, L.A., Patel, S., Garver, J., Gallo, M., Hackett, M., McLaughlin, S., Nadel, M., Harries, J., Gullans, S., Rooke, J., 2006. Nat. Methods 3, 41–46.
Oliveira-Brett, A.M., Diculescu, V., Piedade, J.A.P., 2002. Bioelectrochemistry 55, 61–62.
Palecek, E., Bartosik, M., 2012. Chem. Rev. 112, 3427–3481.
Palecek, E., Fojta, M., 1994. Anal. Chem. 66, 1566–1571.
Qavi, A.J., Kindt, J.T., Gleeson, M.A., Bailey, R.C., 2011. Anal. Chem. 83, 5949–5956.
Ren, Y., Deng, H., Shen, W., Gao, Z., 2013. Anal. Chem. 85, 4784–4789.
Riccelli, P.V., Merante, F., Leung, K.T., Bortolin, S., Zastawny, R.L., Janeczko, R., Benight, A.S., 2001. Nucleic Acids Res. 29, 996–1004.
Schneider, M., Andersen, D.C., Silahtaroglu, A., Lyngbaek, S., Kauppinen, S., Hansen, J.L., Sheikh, S.P., 2011. J. Mol. Histol. 42, 289–299.
Shchepinov, M.S., Case-Green, S.C., Southern, E.M., 1997. Nucleic Acids Res. 25, 1155–1161.
Shi, R., Chiang, V.L., 2005. BioTechniques 39, 519–525.
Sipova, H., Zhang, S., Dudley, A.M., Galas, D., Wang, K., Homola, J., 2010. Anal. Chem. 82, 10110–10115.
Thum, T., Gross, C., Fielder, J., Fischer, T., Kissler, S., Bussen, M., Galuppo, P., Just, S., Rottbauer, W., Frantz, S., Castoldi, M., Soutschek, J., Koteliansky, V., Rosenwald, A., Basson, M.A., Licht, J.D., Pena, J.T.R., Bauersachs, J., Engelhardt, S., 2008. Nature 456, 980–984.
Trojanowicz, M., 2006. TrAC Trends Anal. Chem. 25, 480–489.
Tu, Y., Li, W., Wu, P., Zhang, H., Cai, C., 2013. Anal. Chem. 85, 2536–2542.
Varallyay, E., Burgyan, J., Havelda, Z., 2008. Nat. Protoc. 3, 190–196.
Wang, G.-l., Zhang, C.-y., 2012. Anal. Chem. 84, 7037–7042.
Wang, J., Kawde, A.N., Musameh, M., 2003. Analyst 128, 912–916.
Wang, J., Lin, Y.H., 2008. TrAC Trends Anal. Chem. 27, 619–626.
Wang, J., Yi, X., Tang, H., Han, H., Wu, M., Zhou, F., 2012. Anal. Chem. 84, 6400–6406.
Xiao, C., Rajewsky, K., 2009. Cell 136, 26–36.
Yang, L., Liu, C., Ren, W., Li, Z., 2012. ACS Appl. Mater. Interfaces 4, 6450–6453.
Yin, B.-C., Liu, Y.-Q., Ye, B.-C., 2012. J. Am. Chem. Soc. 134, 5064–5067.
Yu, Z., Zhu, Y., Zhang, Y., Li, J., Fang, Q., Xi, J., Yao, B., 2011. Talanta 85, 1760–1765.
Zamore, P.D., Haley, B., 2005. Science 309, 1519–1524.
Zhang, G.J., Chua, J.H., Chee, R.E., Agarwal, A., Wong, S.M., 2009a. Biosens. Bioelectron. 24, 2504–2508.
Zhang, X., Jiao, K., Liu, S., Hu, Y., 2009b. Anal. Chem. 81, 6006–6012.
Zhang, Y., Zhang, C.-y., 2011. Anal. Chem. 84, 224–231.